Discrete Switching Host-Parasitoid Model with Gamma-Ricker Growth Concerning Integrated Pest Management

Lirong Liu, Changcheng Xiang*, and Guangyao Tang

Abstract—**A novel discrete switching host-parasitoid model with gamma-Ricker growth concerning integrated pest management (IPM) is proposed and studied, where an economic threshold (ET) is selected as a switching threshold. The existence and stability of equilibria of both subsystems are discussed, and then the various equilibria including real and virtual equilibria of switching system can be addressed according to the definitions. In particular, the distribution regions of regular and virtual equilibria related to two-parameter bifurcation diagram are displayed. The effects of ET and other key parameters on the stability of real equilibria are studied, including multi-attractor coexistence and switching-like behavior once some random perturbations are considered. Most interestingly, the basin attractors are numerically provided and initial sensitivities related to the pest control are also discussed in more detail.**

Index Terms—**Switching host-parasitoid model, IPM, initial sensitivities, multi-attractor coexistence, switching-like behavior.**

I. INTRODUCTION

PEST control has been receiving much attention [1]–[5]. The most important reason is that when the pest population density reaches the economic injury level (EIL) [6], pest outbreaks will occur and lead to serious environmental damage or huge economic losses. For instance, desert locust outbreaks have invaded 11 countries in West Africa and caused severe damage to the environment of agricultural production areas [7]. Fortunately, integrated pest management (IPM) is an effective strategy to prevent pest outbreaks and has been proved by many scholars [6], [8]–[11]. Generally, two main methods have been applied to make the pest density below the EIL. One is chemical methods, such as spraying pesticides [12]. The other is biological strategies, such as releasing natural enemies [13], [14].

The reason why chemical control is an indispensable method of IPM is that spraying pesticides can effectively kill pests so that they do not exceed the EIL. However, when pesticides are assessed, it is essential to recognize that the efficiency of the pesticide may be affected by biological and environmental factors [15]. For example, after several insecticides were applied, predaceous mite Typhlodromus occidentalis Nesbitt (Acarina: Phytosciidae) still survived in

Washington apples [16]. Moreover, chemical pesticides are also not always effective. On the one hand, pests will be resistant for the long-term use of the same insecticide [17]. On the other hand, pest outbreaks may generate delays which are difficult to determine [18]. In addition, continued use of pesticides will also cause environmental pollution.

Biological control is another tactic of an IPM strategy [13], [14], that is, the number of pest population decreases dramatically and continuously after natural enemies are released [19]. For instance, a biological control program was developed to reduce the European green crab and Carcinus maenas and has been guided to use in many areas [20]. Another example is the primary method of weed biocontrol which was used to permanently control pests by introducing and releasing exotic insects, mites, or pathogens [21]. Although weed biocontrol is successful [22], there are still some challenges including the effects of public health and the environment, or the attack of nontarget organisms etc [23], [24]. Therefore, more complex IPM strategies, a combination of biological, chemical and cultural tactics, have been applied to effectively control pests [8], [12], [25].

The ET is a crucial concept related to IPM and depends on the consideration of economy, society or ecology [10]. When the pest population density reaches the ET, IPM measures are applied to reduce the number of pests. Tang et al. aimed to decrease the use of pesticides, so a model containing regular release of natural enemies and chemical control with ET was developed [25].

The dynamical systems with IPM about host-parasitoid were established by the discrete switching systems. Recently, Xiang et al. have studied the host-parasitoid model with respect to Beverton-Holt growth and combined with IPM [26]. Another switching host-parasitoid model with IPM has been studied by Xiang and Tang et al. [27]. In the present paper, based on the Nicholson-Bailey model [28], a discrete switching host-parasitoid model with gamma-Ricker growth concerning IPM is constructed and analyzed. The existence of equilibria of the proposed system is not only addressed by constructing auxiliary functions, but is confirmed by numerical simulation. Then, the stable conditions for equilibria of the switching system are discussed, and four possible cases are investigated. Moreover, three cases for the coexistence of equilibria of the system are also discussed.

The bifurcation diagrams of crucial parameters are displayed and analyzed. According to the bifurcation analysis, the system has various dynamics. On the one hand, we address how initial sensitivities affect the final states of these two populations and the number of the host outbreaks. On the other hand, the influence of different parameters on the

switching-like behavior is discussed by adding some random perturbations.

The main structure of this paper is as follows: in Section 2, a discrete switching host-parasitoid model with gamma-Ricker growth is proposed, and an ET is selected as the switching threshold. In Section 3, the existence and stability of equilibria of the proposed system are analyzed. What's more, the two-parameter bifurcation diagram is used to display the coexistence of different equilibria. In Section 4, numerical investigations of the system are shown. The bifurcation analysis reveals the existence and coexistence of multiple attractors, initial sensitivities and switching-like behavior. The question of how the factors affect the host population outbreaks is addressed, which includes the crucial parameters and initial densities of host and parasitoid populations. The conclusion is drawn in Section 5.

II. MODEL DESCRIPTION

The famous gamma-Ricker model [29] was given by

$$H_{t+1} = \beta H_t^{\gamma} e^{-\delta H_t}, t = 1, 2, 3, ..., \tag{1}$$

where H_t is the host population density in generation t ($t = 1, 2, 3, ...$). β, γ and δ are positive real parameters. The simplest gamma-Ricker model has been used to explore the factors that affect positive and negative density dependence [29]. γ denotes the intrinsic growth rate of the host population, and the main results revealed that when $\gamma > 1$, the per-capita growth rate of the population combines both negative and positive dependence. When $\gamma \leq 1$, the population is overcompensatory. Hence, we are concerned about the effects of γ on the host population in model (1).

Under the consideration of parasitoid's interference to host and interactions between them, based on the classical Nicholson−Bailey model [28], model (2) is derived from model (1) and rewritten as

$$\begin{cases} H_{t+1} = \beta H_t^{\gamma_1} e^{-\delta H_t - \alpha P_t} \triangleq Q_{11}(H, P), \\ P_{t+1} = \beta H_t^{\gamma_1}(1 - e^{-\alpha P_t}) \triangleq Q_{12}(H, P), \end{cases} \tag{2}$$

where $e^{-\alpha P_t}$ means the escape rate of the host population fleeing from the parasitoid population, β is a positive constant, the intrinsic growth rate and mortality rate of the host population are denoted by γ_1 and $e^{-\delta H_t}$, respectively. From a biological point of view, the host and parasitoid populations are also taken as pests (prey) and natural enemies (predators).

Based on model (2), when the host population density is greater than the value of ET, the chemical and biological control measures are applied. On the one hand, the use of pesticides has impacts on the growth rates of both host population and parasitoid population. So we assume that $\gamma_2 < \gamma_1$ always holds, where γ_2 is the growth rate of the host population after spraying pesticides. On the other hand, the release of natural enemies is taken, when the number of the host population is over the ET. Ultimately, the purpose of IPM strategies is achieved. So model (2) with IPM strategies is written as follows:

$$\begin{cases} H_{t+1} = (1-p)\beta H_t^{\gamma_2} e^{-\delta H_t - \alpha P_t} \triangleq Q_{21}(H, P), \\ P_{t+1} = \beta H_t^{\gamma_2}(1 - e^{-\alpha P_t}) + \tau \triangleq Q_{22}(H, P), \end{cases} \tag{3}$$

where p ($0 \leq p < 1$) is the killing rate and τ ($\tau \geq 0$) is the number of releasing natural enemies. Thus combining the control measures, there are three possible cases.

- If $p > 0$ and $\tau = 0$, then only the chemical control tactics (i.e., spraying pesticides) are adopted to control pests.
- If $p = 0$ and $\tau > 0$, then only the biological control measures (i.e., releasing natural enemies) are taken to make the number of pests fall the ET.
- If $p\tau \neq 0$, then both chemical and biological control measures are considered.

Therefore, combining with models (2) and (3), we have the following ET guided switching system.

$$\begin{cases} \left. \begin{array}{l} H_{t+1} = \beta H_t^{\gamma_1} e^{-\delta H_t - \alpha P_t}, \\ P_{t+1} = \beta H_t^{\gamma_1}(1 - e^{-\alpha P_t}), \end{array} \right\} H_t < ET, \\ \left. \begin{array}{l} H_{t+1} = (1-p)\beta H_t^{\gamma_2} e^{-\delta H_t - \alpha P_t}, \\ P_{t+1} = \beta H_t^{\gamma_2}(1 - e^{-\alpha P_t}) + \tau, \end{array} \right\} H_t \geq ET. \end{cases} \tag{4}$$

The switching systems have been widely applied [30]–[32]. In the present work, the switching model (4) is valued. We aim to address the existence and stability of equilibria of the system, and investigate the effects of ET and other key parameters on the stability of real equilibria by means of one- or two-parameter bifurcation. Moreover, some complex dynamic behaviors and actual biological implications are explored through the bifurcation analysis.
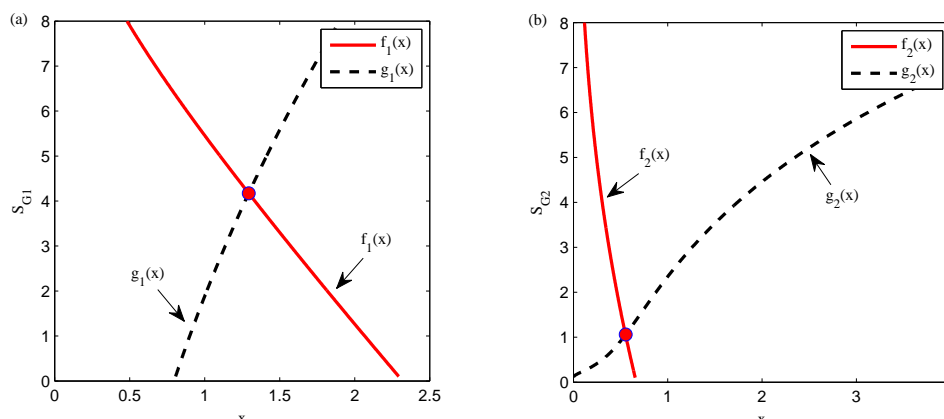

Fig. 1. Existence of equilibra of subsystems S_{G1} and S_{G2}.

III. EQUILIBRIA AND THEIR STABILITY OF THE SWITCHING SYSTEM

For convenience, $F(H(t)) = H(t) - ET$ and $Z(t) = [H(t), P(t)]^T$ are denoted, so system (4) is rewritten as

$$S_{G_1}(t+1) = \begin{bmatrix} \beta H(t)^{\gamma_1} e^{-\delta H(t) - \alpha P(t)} \\ \beta H(t)^{\gamma_1}(1 - e^{-\alpha P(t)}) \end{bmatrix},$$

(5)

$$S_{G_2}(t+1) = \begin{bmatrix} (1-p)\beta H(t)^{\gamma_2} e^{-\delta H(t) - \alpha P(t)} \\ \beta H(t)^{\gamma_2}(1 - e^{-\alpha P(t)}) + \tau \end{bmatrix},$$

where G_1 and G_2 are two different regions that are defined as follows:

$$\begin{aligned} G_1 &= \{(H, P) | F(H) < 0, H > 0, P > 0\}, \\ G_2 &= \{(H, P) | F(H) \geq 0, H > 0, P > 0\}. \end{aligned}$$

(6)

In this paper, subsystem S_{G1} in region G_1 and subsystem S_{G2} in region G_2 of system (5) are defined. To discuss the different types of equilibria for system (5), the existence and stability of equilibria are addressed in the following.

A. Equilibria of the switching subsystems S_{G1} and S_{G2}

For subsystem S_{G1}, let $H_t = H_{t+1} = H_{1*}$, and $P_t = P_{t+1} = P_{1*}$. Then the equilibrium $E_{1*} = (H_{1*}, P_{1*})$ satisfies two equations:

$$\begin{aligned} H_{1*} &= \beta H_{1*}^{\gamma_1} e^{-\delta H_{1*} - \alpha P_{1*}}, \\ P_{1*} &= \beta H_{1*}^{\gamma_1}(1 - e^{-\alpha P_{1*}}). \end{aligned}$$

(7)

It is evident that there is an extinction steady state $E_{00} = (0,0)$, and (7) consists of two transcendental equations. To address the existence of E_{1*}, two additional functions are constructed as

$$\begin{aligned} f_1(x) &= W_1^{\frac{1}{\gamma_1}}, \\ g_1(x) &= \frac{1}{\delta}(\ln\beta + \ln W_1^{\frac{\gamma_1 - 1}{\gamma_1}} - \alpha x), \end{aligned}$$

(8)

where $W_1 = \frac{x}{\beta - \beta e^{-\alpha x}}$. If $x > 0$ and $f_1(x) = g_1(x)$ hold, then E_{1*} exists in subsystem S_{G1}.

Analogously, for subsystem S_{G2}, let $H_t = H_{t+1} = H_{2*}$, and $P_t = P_{t+1} = P_{2*}$. Then the equilibrium $E_{2*} = (H_{2*}, P_{2*})$ satisfies

$$\begin{aligned} H_{2*} &= (1-p)\beta H_{2*}^{\gamma_2} e^{-\delta H_{2*} - \alpha P_{2*}}, \\ P_{2*} &= \beta H_{2*}^{\gamma_2}(1 - e^{-\alpha P_{2*}}) + \tau. \end{aligned}$$

(9)

Let

$$\begin{aligned} f_2(x) &= W_2^{\frac{1}{\gamma_2}}, \\ g_2(x) &= \frac{1}{\delta}(\ln(1-p)\beta + \ln W_2^{\frac{\gamma_2 - 1}{\gamma_2}} - \alpha x), \end{aligned}$$

(10)

where $W_2 = \frac{x-\tau}{\beta - \beta e^{-\alpha x}}$. Similarly, if $x > 0$ and $f_2(x) = g_2(x)$ are true, then subsystem S_{G2} has an equilibrium E_{2*}.

To verify the existence of equilibria of these two subsystems by employing numerical simulation, Fig.1(a) and Fig.1(b) are plotted. The parameters are $\beta = 6$, $\alpha = 0.2$, $\delta = 0.7$, $p = 0.8$, $\tau = 0.1$, $\gamma_1 = 0.8$ and $\gamma_2 = 0.3$.

B. Stability of the equilibrium of switching system (5)

For subsystem S_{G1}, the local stability of E_{1*} is determined by the eigenvalues of Jacobian matrix as follows:

$$J = \begin{pmatrix} \partial Q_{11}/\partial H & \partial Q_{11}/\partial P \\ \partial Q_{12}/\partial H & \partial Q_{12}/\partial P \end{pmatrix}.$$

(11)

According to equation (5), we have

$$J_1 = \begin{pmatrix} \beta A^{\gamma_1 - 1} e^{-\delta A} B(\gamma_1 - \delta A) & -\alpha\beta A^{\gamma_1} e^{-\delta A} B \\ \beta\gamma_1 A^{\gamma_1 - 1}(1 - B) & \alpha\beta A^{\gamma_1} B \end{pmatrix},$$

(12)

where

$$A = \left(\frac{P_{1*}}{\beta - \beta e^{-\alpha P_{1*}}}\right)^{\frac{1}{\gamma_1}}, \quad B = e^{-\alpha P_{1*}}.$$

(13)

Its characteristic equation is

$$Q(\lambda) = \lambda^2 - Trace(J_1)\lambda + Det(J_1),$$

(14)

where

$$Trace(J_1) = \beta A^{\gamma_1 - 1} B\left(e^{-\delta A}(\gamma_1 - \delta A) + \alpha A\right),$$
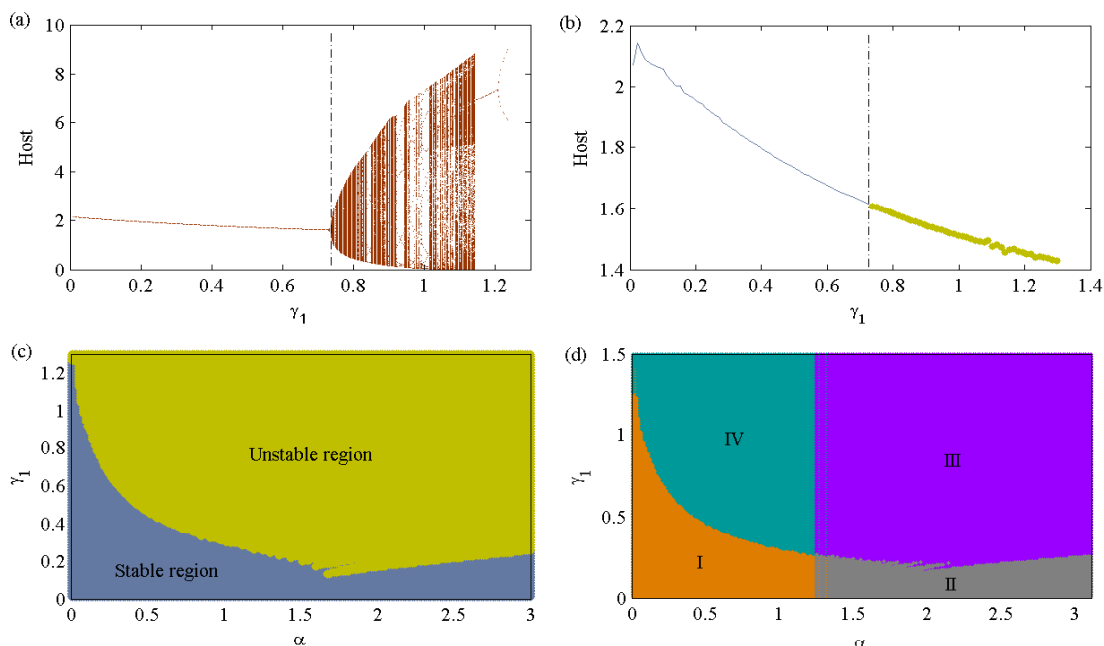
(15)

Fig. 2. Stability of equilibria of system (5).

$$Det(J_1) = \alpha\beta^2 A^{2\gamma_1-1}e^{-\delta A}B\left(\gamma_1 - \delta AB\right). \qquad (16)$$

According to the Jury criteria [33], [34], if E_{1*} satisfies the local stability conditions, namely,

$$|Trace(J_i)| < 1 + Det(J_i) < 2 \quad (i = 1, 2), \qquad (17)$$

then E_{1*} is locally asymptotically stable. Similarly, if E_{2*} satisfies (17), then E_{2*} is also locally asymptotically stable.

Furthermore, there is an interesting problem about the stability of equilibria for subsystems S_{G1} and S_{G2} in the parameter space $\alpha - \gamma_1$. The parameters are $\beta = 6$, $\delta = 0.3$, $p = 0.3$, $\tau = 0.1$ and $\gamma_2 = 0.3$. When $\alpha = 0.2$, Fig.2(a) shows the bifurcation diagram of subsystem S_{G1} with respect to parameter γ_1. When $\gamma_1 \in (0, 0.73)$, E_{1*} is stable. When $\gamma_1 \in (0.73, 1.2)$, E_{1*} is unstable and subsystem S_{G1} is in a chaotic state. Fig.2(b) shows the stability of E_{1*}, where thin dots indicates stable E_{1*} and thick dots indicates unstable E_{1*}. In particular, it is completely consistent with the results shown in Fig.2(a). In Fig.2(c), for subsystem S_{G1}, the parameter space $\alpha - \gamma_1$ is divided into stable region and unstable region. Fig.2(d) shows that the parameter space $\alpha - \gamma_1$ has four regions for the whole switching system (5) and is denoted by I, II, III, IV, respectively. In region I, E_{1*} and E_{2*} are stable. In region II, E_{1*} is stable, E_{2*} is unstable. In region III, E_{1*} is unstable, E_{2*} is stable. In region IV, E_{1*} and E_{2*} are unstable.

C. Equilibria of switching system (5)

Regular and virtual equilibria of system (5) are discussed, and their definitions are introduced in the following.

Definition 3.1: $E_{i*} = (H_{i*}, P_{i*})(i = 1, 2)$ is called a regular equilibrium of system (5), if $F(H_{1*}) < 0$ or $F(H_{2*}) \geq 0$, these equilibria are denoted by $E_{S_{G1}}^R$ and $E_{S_{G2}}^R$, respectively. E_{i*} is called a virtual equilibrium of system (5), if $F(H_{1*}) \geq 0$ or $F(H_{2*}) < 0$, these equilibria

are denoted by $E_{S_{G1}}^V$ and $E_{S_{G2}}^V$, respectively.

To display the coexistence of different equilibria for these two subsystems, we plot the α-ET parameter space diagram and other parameters are $\beta = 6$, $\alpha = 0.2$, $\delta = 0.7$, $p = 0.3$, $\tau = 0.1$, $\gamma_1 = 0.8$ and $\gamma_2 = 0.3$. The solid circles represent E_{1*}, and the hollow circles represent E_{2*} [see Fig.3((a)-(c))]. The results show that H_{1*} is always greater than H_{2*}, then the following three cases of the coexistence of equilibria are discussed.

(i) If $ET > H_{1*} > H_{2*}$, then $E_{S_{G1}}^R$ and $E_{S_{G2}}^V$ coexist.
(ii) If $H_{1*} \geq ET > H_{2*}$, then $E_{S_{G1}}^V$ and $E_{S_{G2}}^V$ coexist.
(iii) If $H_{1*} > H_{2*} \geq ET$, then $E_{S_{G1}}^V$ and $E_{S_{G2}}^R$ coexist.

Letting the range of α be $[0.1, 0.6]$, and ET changes in $[0.5, 2.5]$, it is clear that the α-ET parameter space is divided into three regions [see Fig.3(d)]. In region I, $E_{S_{G1}}^R$ and $E_{S_{G2}}^V$ coexist. In region II, $E_{S_{G1}}^V$ and $E_{S_{G2}}^V$ coexist. In region III, $E_{S_{G1}}^V$ and $E_{S_{G2}}^R$ coexist.

From Fig.3, with the variation of one or more parameters, the results changes significantly. The main purpose of a suitable pest control strategy is to prevent the pest outbreaks, that is, the pest population density does not exceed the ET. As far as the perspective of the mathematical view, the system is stable at the desired level by employing IPM strategies. Thus, in terms of IPM, the right value of ET should be considered to make the equilibria of both subsystem S_{G1} and subsystem S_{G2} become virtual.

IV. NUMERICAL ANALYSIS OF MODEL (5)

This section provides numerical simulations for system (5). In particular, the existence and coexistence of multiple attractors, initial sensitivities and switching-like behavior are revealed by the bifurcation analysis.

A. Bifurcation analysis

To get some basic properties of the dynamical system, one-parameter bifurcation diagrams for γ_1 (i.e., the intrinsic
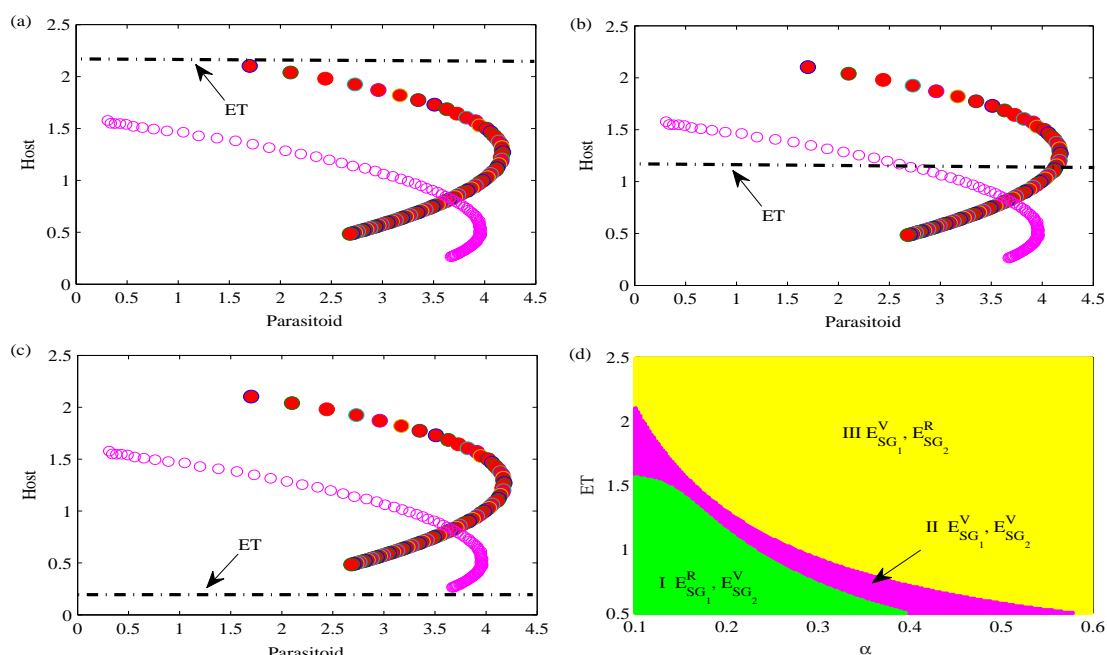
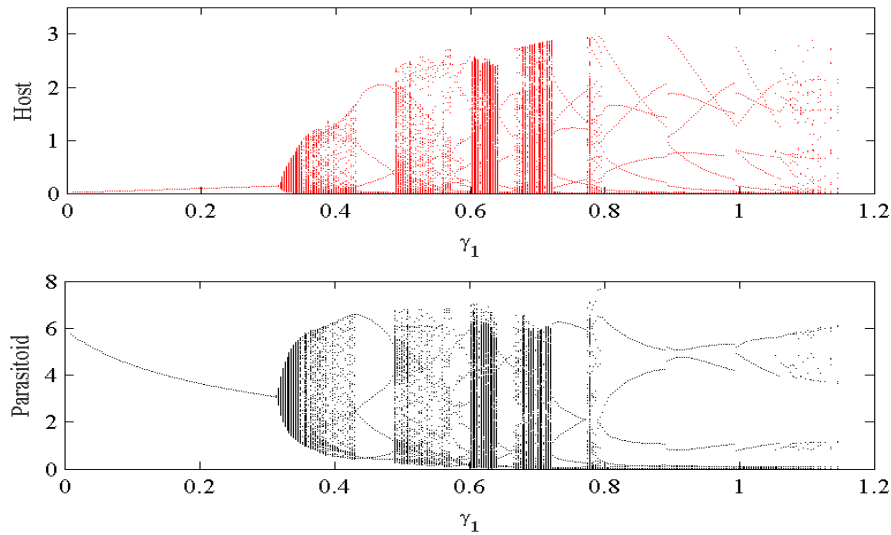

Fig. 3. Coexistence of different equilibria of system (5).

Fig. 4. Bifurcation diagrams about γ_1 of system (5).

growth rate of the host population) and p (i.e., killing rate) are analyzed. The results reveal the existence of different attractors with the change of parameter γ_1.

Parameter γ_1 is first selected as the bifurcation parameter. Other parameters are $\beta = 6$, $\alpha = 1$, $\delta = 0.7$, $ET = 1$, $p = 0.28$ and $\tau = 0.1$. The initial value is $(H_0, P_0) = (0.8, 0.5)$. In Fig.4, the range of γ_1 is $(0, 1.2)$, system (5) has many complex dynamics, such as multi-attractor coexistence, chaotic bands and chaos crisis. Obviously, when $\gamma_1 \in (0, 0.43)$, the system goes from a stable state to a chaotic state. With the further increase of γ_1, multiple periods appear. In particular, there are multiple attractors in $[0.7, 0.8]$ or $[1, 1.2]$.

Fig.5 shows the bifurcation diagrams about parameter p. Other parameters are $\beta = 7.7$, $\alpha = 0.34$, $\delta = 1.305$, $ET = 1$, $\tau = 0.8$, $\gamma_1 = 0.7972$ and $\gamma_2 = 0.558$. The initial value is $(H_0, P_0) = (0.5, 0.4)$. When killing rates of pesticides are too small or too large, the host outbreaks will occur. It means

that the host population density is above the ET. For example, when $p \in (0, 0.18)$ or $(0.74, 1]$, the host outbreaks will occur. Interestingly, Fig.5 clearly reveals that the appropriate killing rate is selected to make system (5) stable in subsystem S_{G_1}. That is, when $p \in [0.18, 0.74)$, the host outbreaks will not generate.

B. Initial sensitivities

Different initial densities of the host and parasitoid populations lead to different outbreak modes and also affect the coexistence of multiple attractors. Therefore, the influence of initial densities on their final states, host-outbreak modes and the outcome of successful pest control are emphasized. The coexistence of multiple attractors is discussed in the following subsection.

Parameter p is selected as 0.3, and other parameters are the same as those of Fig.5. In Fig.6(a), the densities of these two populations always do not exceed the ET, and
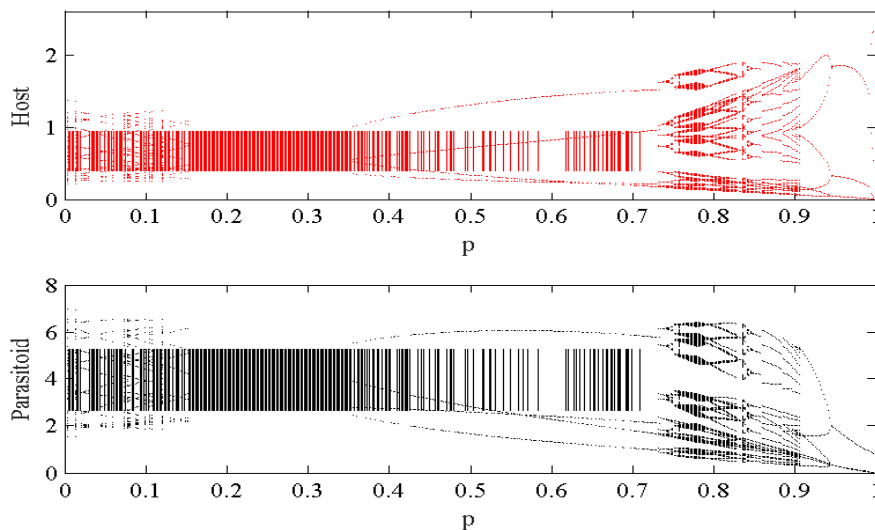

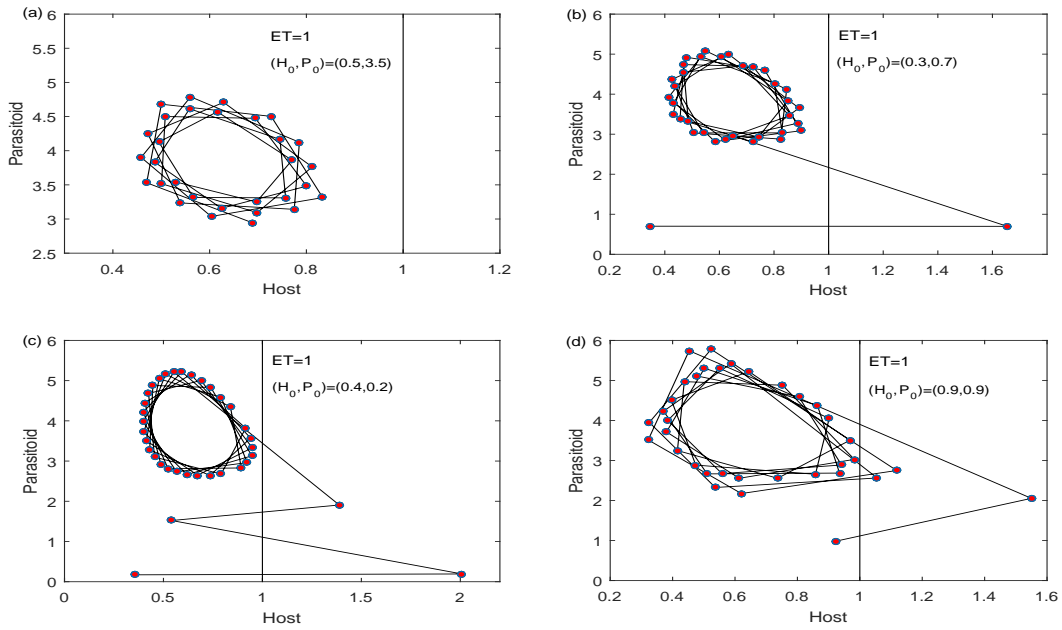Fig. 5. Bifurcation diagrams about p of system (5).

Fig. 6. Influence of initial densities of these two populations on switching frequencies for system (5).

their initial densities are 0.5299, 3.5430. This case shows that no measures need to be taken. Fig.6(b) indicates that one IPM strategy is required to make initial density of the host population not cross the ET. If the values of initial densities are $(0.3588, 0.1718)$ or $(0.9232, 0.9841)$, then the results indicate that the pests can be controlled after two or three IPM measures [see Fig.6(c) or (d)]. Fig.6 shows that these two populations are stable in subsystem S_{G_1} after taking zero, one, two or three IPM tactics.

To further discuss the effects of their initial values on host-outbreak frequencies, Fig.7 with different p is plotted. Other parameters are the same as those of Fig.5. The central region is denoted by 'Nonoutbreak region', where the pest (host) population never outbreaks. Meanwhile, there is no need to take any IPM strategy. In regions II III and IV, where the host population could be controlled after one, two, three control strategies are applied. Moreover, in region I, where pests experience multiple outbreaks. So when different values of p are taken, the number of control measures required to be stable in subsystem S_{G_1} is different. For instance, if $p = 0.1$ [see Fig.7(a)], control tactics are taken up to two times to make host population stable in subsystem S_{G_1}. If $p = 0.3$ [see Fig.7(b)], the host population is stable in subsystem S_{G_1} after applying four control strategies. If $p = 0.55$
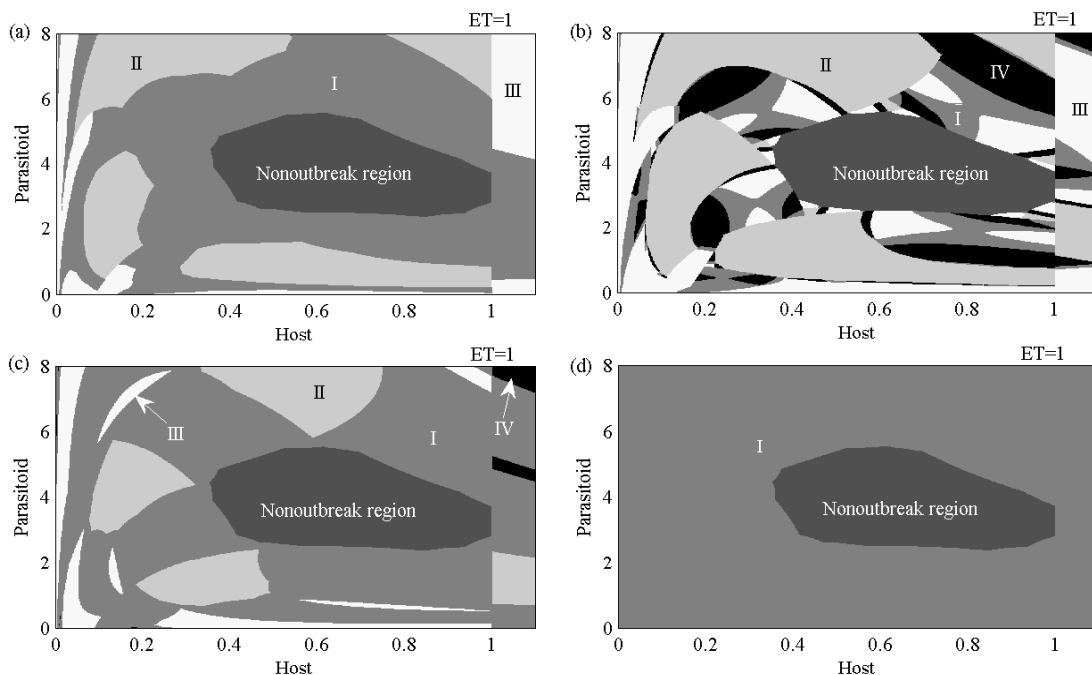

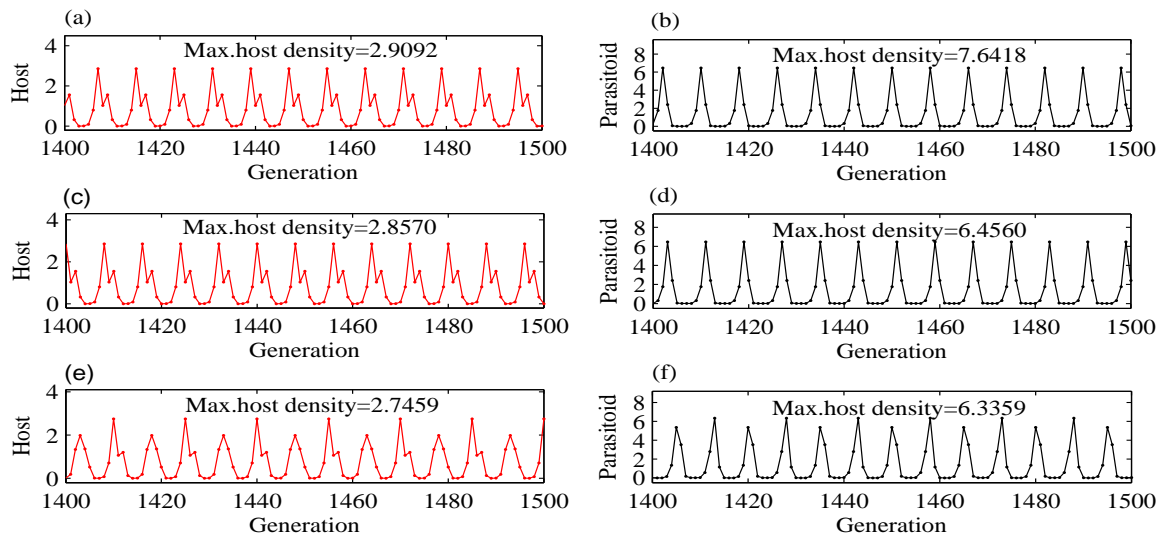Fig. 7. The impacts of different values of p on host-outbreak frequencies.

Fig. 8. Coexistence of three attractors with different initial values for system (5).

[see Fig.7(c)], three control tactics are need to make the host population stable in subsystem S_{G_1}. If $p = 0.75$ [see Fig.7(d)], region I represents that the host outbreaks occur many times. Additionally, the results indicate that initial values of these two populations may affect their final states.

C. Multiple attractors and coexistence

As mentioned above, model (5) reveals many dynamic behaviors, in particular, the coexistence of multiple attractors is contained. In order to confirm that initial densities of these two populations how to affect the host outbreaks and the implementation of control tactics, Fig.8 is plotted. Some parameters are the same as those of Fig.4. When $\gamma_1 = 0.7972, \gamma_2 = 0.558$, there exists the coexistence of three attractors, and each attractor has the different amplitudes and frequencies. If the initial value is set as $(H_0, P_0) = (2.3, 3.15)$, then Fig.8((a)-(b)) oscillate with period 33, and the solution of system (5) approaches the first attractor. The maximum amplitudes of host and parasitoid

populations are 2.9092, 7.6418, respectively. If the initial value is $(H_0, P_0) = (3.7, 2.9)$, then the second attractor is shown in Fig.8((c)-(d)). The last attractor has the smallest amplitudes and the initial value is $(H_0, P_0) = (3.5, 3)$ as shown in Fig.8((e)-(f)). The maximum amplitudes of host and parasitoid populations are 2.7459, 6.3359, respectively.

When $\gamma_1 = 1.104, \gamma_2 = 0.773$, three attractors coexist. Other parameters are the same as those of Fig.4. The coexistence of the other three attractors is shown in Fig.9. The result indicates that different attractors have different oscillation modes, that is, amplitudes and frequencies of different attractors are different.

Fig.8 and Fig.9 indicate that the IPM strategies are effectively employed to reduce the host population density, which depends on the initial densities of these two populations being well monitored and tracked. In Fig.10, the basins of attraction about the coexistence of these multiple attractors are shown. The initial densities of host and parasitoid populations are the horizontal and vertical axes, respectively. As
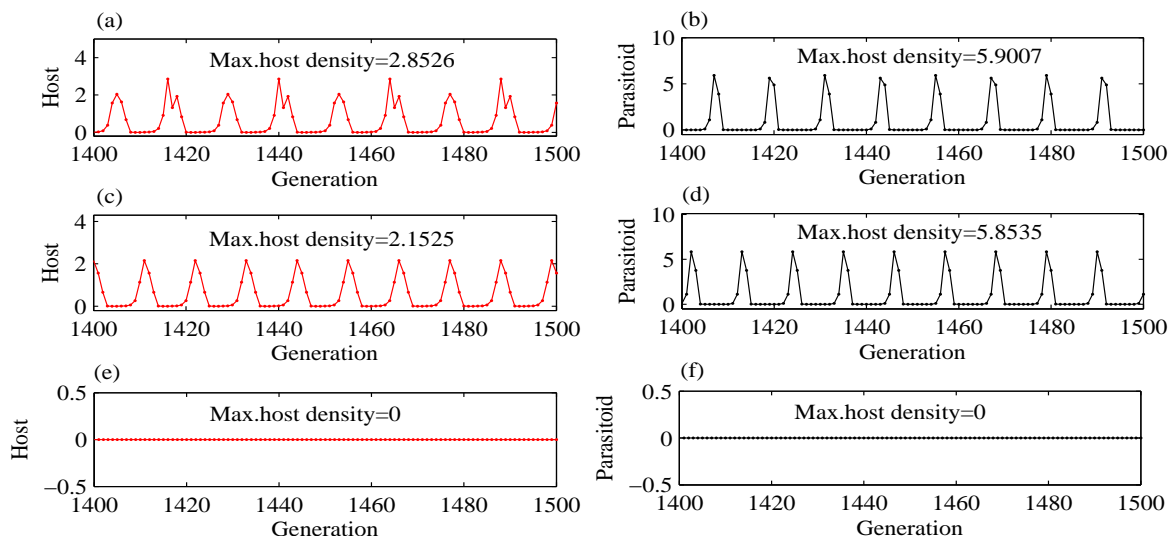

Fig. 9. Coexistence of three attractors with different initial values for system (5).
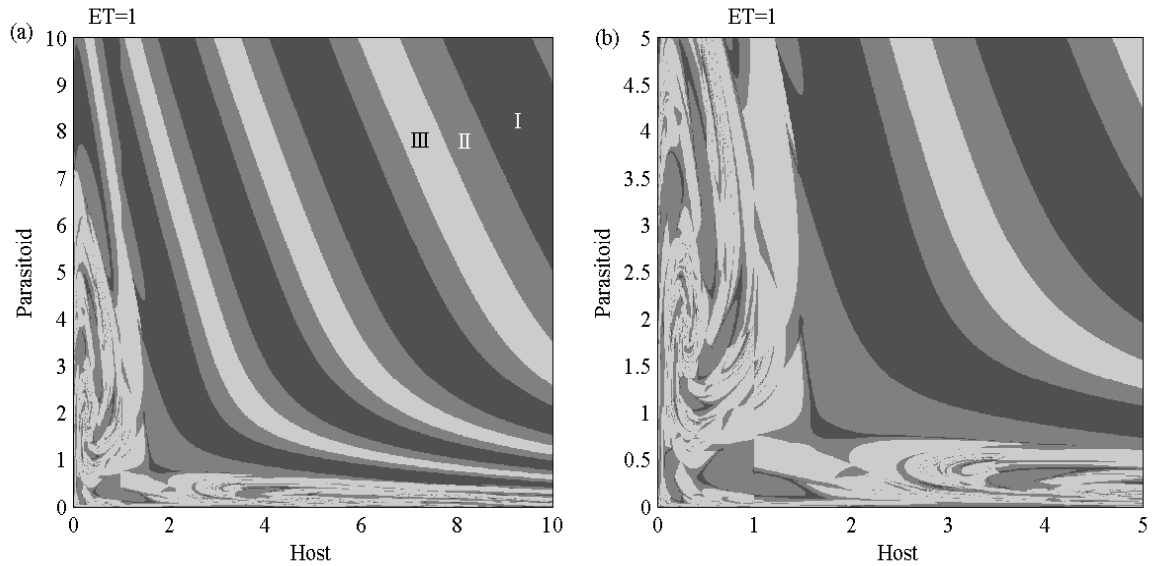
Fig. 10. Basins of attraction of multi-attractor coexistence for system (5).

shown in Fig.10(a), the ranges of initial densities of two populations are $0 \leq H_0 \leq 10$, $0 \leq P_0 \leq 10$. Fig.10(b) is the coordinate of Fig.10(a) expanding the range to $0 \leq H_0 \leq 5$, $0 \leq P_0 \leq 5$. Fig.10 displays the basins of attraction for three attractors denoted by I II and III. Three regions correspond to three periodic solutions shown in Fig.8, respectively.

Fig.11 shows the basins of attraction of another case where three attractors coexist. These periodic solutions of the regions are shown in Fig.9. In particular, Fig.10 and Fig.11 show that there is a clear block that is a so-called fractal property about self-similarity, and the fractal boundary is exactly $ET = 1$.

D. Switching-like behavior

So as to comprehend how the population density of parasitoid affects the ultimate state of the host population,

subsystem S_{G_2} is rewritten as follows

$$S_{G_2}(\mathrm{t}+1) = \left[\begin{array}{c} (1-p)\beta H(t)^{\gamma_2} e^{-\delta H(t) - \alpha P(t)} \\ \beta H(t)^{\gamma_2}(1 - e^{-\alpha P(t)}) + \tau_t \end{array} \right], \quad (18)$$

where at generation t, $\tau_t = \tau$, i.e., there is not the random perturbation. Or $\tau_t = \tau + \sigma u$, i.e., there exists the random perturbation, where $u \in [-1, 1]$, σ denotes the noise intensity and is a positive constant. We aim to address the effects of the noise intensity on the stable attractor.

To do this, the initial value is fixed as $(H_0, P_0) = (3, 3.1)$, and the rest of parameters are the same as those of Fig.8. In Fig.12, if $\sigma = 0.85$ is added at every 200 generations, then the switching-like behavior of the attractors occurs. When $t \in [0, 200)$, the first attractor is stable. Once $t = 200$, the random perturbation is added, and the system switches to the second stable attractor with smaller amplitude. When $t =$
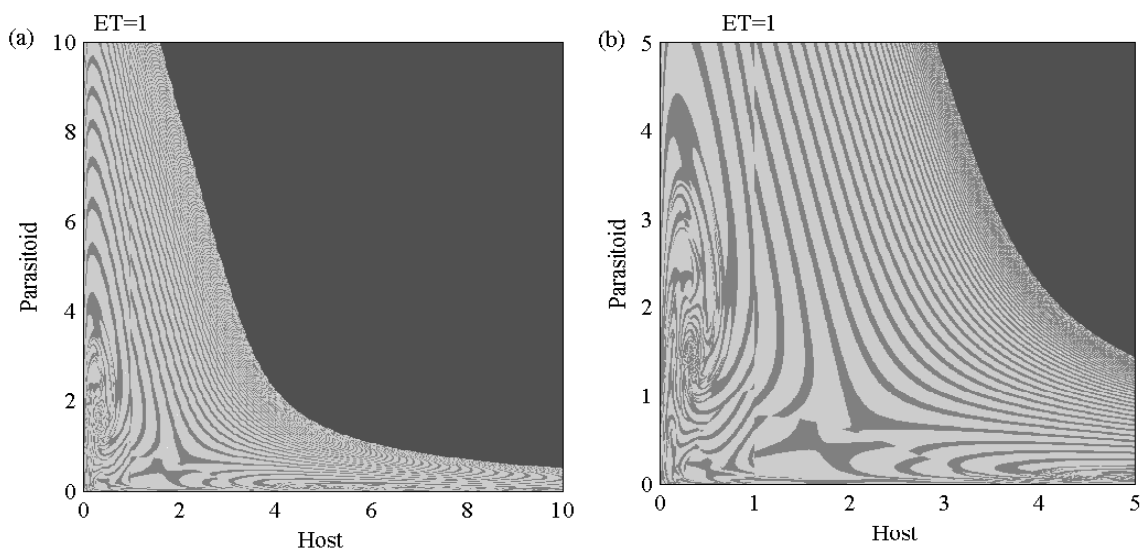

Fig. 11. Basins of attraction of multi-attractor coexistence for system (5).
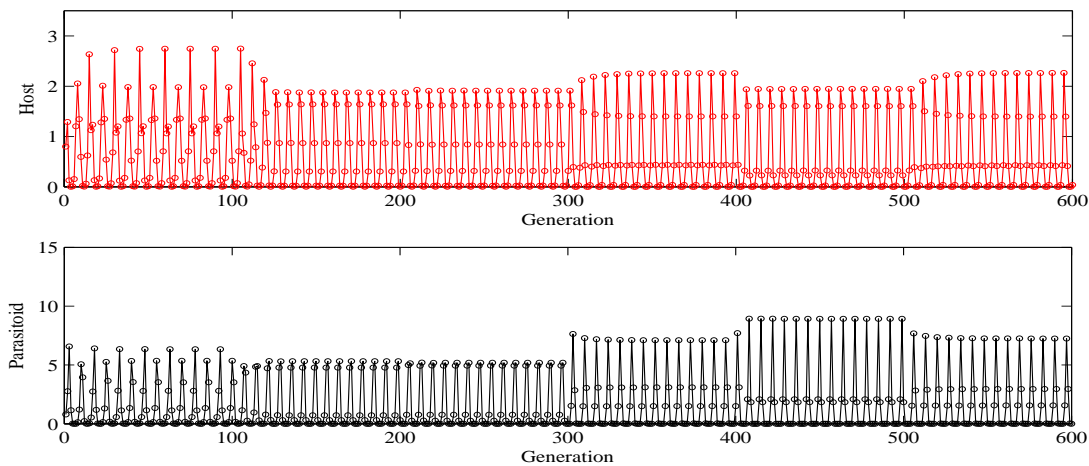
Fig. 12. Switching-like behavior of multiple attractors for system (5).

400, the second stable attractor switches to another stable attractor with larger amplitude.

To address the issue of how different killing rates affect the switching-like behavior of host and parasitoid populations, subsystem S_{G_2} is rewritten as follows

$$S_{G_2}(\text{t}+1) = \begin{bmatrix} (1-p_t)\beta H(t)^{\gamma_2} e^{-\delta H(t) - \alpha P(t)} \\ \beta H(t)^{\gamma_2}(1 - e^{-\alpha P(t)}) + \tau \end{bmatrix}, \quad (19)$$

where p_t is the random perturbation function about p at generation t. If there is not the random perturbation, then $p_t = p$. If there exists the random perturbation, then $p_t = p + \eta u$ and $\eta > 0$ (i.e., noise intensity). From Fig.13, $\eta = 0.75$, at every 200 generations, and the rest of parameters are the same as those of Fig.8. When the killing rate has the random perturbation with larger intensity, the similar switching-like behavior occurs.

V. Conclusion

A novel discrete switching host-parasitoid model with gamma-Ricker growth concerning IPM based on the classical Nicholson-Bailey model is proposed. The system has two subsystems (S_{G_1} and S_{G_2}) and is guided to switch by the ET. In particular, S_{G_1} is a system without control and S_{G_2} is a control system.

The existence of equilibria of the proposed system is addressed by constructing auxiliary functions as shown in Fig.1. Then, the stable conditions of equilibria of the system are discussed, and the two-parameter bifurcation diagrams are also displayed in Fig.2. Four possible cases of subsystems S_{G_1} and S_{G_2} are as follows. (i) Subsystems S_{G_1} and S_{G_2} are stable. (ii) Subsystem S_{G_1} is stable, subsystem S_{G_2} is unstable. (iii) Subsystem S_{G_1} is unstable, subsystem S_{G_2} is stable. (iv) Subsystems S_{G_1} and S_{G_2} are unstable. Moreover, three cases for the coexistence of equilibria of system (5) are also discussed. They are $ET > H_{1*} > H_{2*}$ [see Fig.3(a)], $H_{1*} \geq ET > H_{2*}$ [see Fig.3(b)] and $H_{1*} > H_{2*} \geq ET$ [see Fig.3(c)], respectively. These three types of equilibria coexistence are shown in Fig.3(d). Thus, as far as the perspective of IPM, to make the equilibria of subsystems S_{G_1} and S_{G_2} become virtual simultaneously, the ET should be considered.

The bifurcation diagrams about killing rate p show that $p \in [0.18, 0.74)$, the host population outbreaks will not occur [see Fig.5]. Moreover, the different initial densities of pests and natural enemies affect their final states [see Fig.6]. From
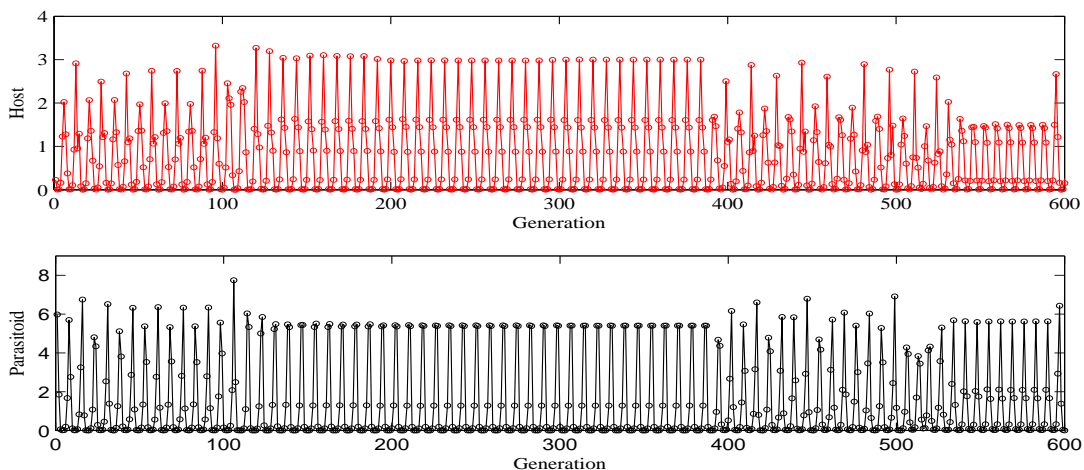

Fig. 13. Switching-like behavior of multiple attractors for system (5).

Fig.6, the host population is stable in subsystem S_{G_1} after zero, one, two or three IPM measures are applied. The results show that the different initial densities and ratios of pests and natural enemies lead to various ultimate states of these two populations.

The bifurcation diagrams with respect to the intrinsic growth rate of the host population γ_1 indicate that system (5) has various dynamics as shown in Fig.4. When $\gamma_1 \in [0.7, 0.8]$ or $[1, 1.2]$, the coexistence of three kinds of attractors and switching-like behavior occur. To investigate this, γ_1 is set as 0.7972 or 1.104, the other parameters are fixed as those of Fig.4. The results reveal that these different attractors with different initial densities have different amplitudes and switching frequencies [see Fig.8 and Fig.9]. Therefore, the choices of IPM control tactics are strictly dependent on initial densities of both host and parasitoid populations. In Fig.10 and Fig.11, the basins of attraction are used to present the coexistence of these multiple attractors. Random perturbations of τ and p added are applied to address the influence of different τ and p on the switching-like behavior. The results indicates that the stable attractor could switch from one attractor to another attractor.

This work concentrated on the discrete switching host-parasitoid model with gamma-Ricker growth about IPM tactics and the mutual effects of both host and parasitoid populations. In the future, the general or Holling type functional responses of parasitoid population [35]–[37], a host-parasitoid model with time delay [38] could be considered.

REFERENCES

[1] M. Grainge, *Handbook of plants with pest-control properties*. Resource Systems Institute, East-West Center, Wiley, 1988.

[2] R. Naylor and P. R. Ehrlich, "Natural pest control services and agriculture," *Nature's Services: societal dependence on natural ecosystems*, pp. 151–174, 1997.

[3] J. R. Thacker, *An introduction to arthropod pest control*. Cambridge University Press, UK, 2002.

[4] P. K. Dearden *et al.*, "The potential for the use of gene drives for pest control in new zealand: a perspective," *Journal of the Royal Society of New Zealand*, vol. 48, no. 4, pp. 225–244, 2018.

[5] A. Wieser, F. Reuss, A. Niamir, R. Müller, R. B. OHara, and M. Pfenninger, "Modelling seasonal dynamics, population stability, and pest control in aedes japonicus japonicus (diptera: Culicidae)," *Parasites & vectors*, vol. 12, no. 1, pp. 142–153, 2019.

[6] S. Tang, Y. Xiao, and R. A. Cheke, "Multiple attractors of host parasitoid models with integrated pest management strategies: Eradication, persistence and outbreak," *Theoretical Population Biology*, vol. 73, no. 2, pp. 181–197, 2008.

[7] C. Pietro, C. Keith, G. Alessandra, and T. Sylwia, "The desert locust upsurge in west africa (2003 - 2005): Information on the desert locust early warning system and the prospects for seasonal climate forecasting," *PANS Pest Articles & News Summaries*, vol. 53, no. 1, pp. 7–13, 2007.

[8] S. Tang and R. A. Cheke, "Models for integrated pest control and their biological implications," *Mathematical Biosciences*, vol. 215, no. 1, pp. 115–125, 2008.

[9] M. I. Costa and L. B. Faria, "Integrated pest management: theoretical insights from a threshold policy," *Neotropical Entomology*, vol. 39, no. 1, pp. 1–8, 2010.

[10] L. G. Higley and L. P. Pedigo, *Economic thresholds for integrated pest management*. University of Nebraska Press, US, 1996.

[11] J. Liang, S. Tang, and R. A. Cheke, "A discrete host-parasitoid model with development of pesticide resistance and ipm strategies," *Journal of Biological Dynamics*, vol. 12, no. 1, pp. 1059–1078, 2018.

[12] C. Xiang, Z. Xiang, S. Tang, and J. Wu, "Discrete switching host-parasitoid models with integrated pest control," *International Journal of Bifurcation & Chaos*, vol. 24, no. 9, p. 1450114, 2014.

[13] F. D. Parker, *Management of Pest Populations by Manipulating Densities of Both Hosts and Parasites Through Periodic Releases*. Springer, US, 1971.

[14] N. Helyer, N. D. Cattlin, N. Helyer, and N. D. Cattlin, "Biological control in plant protection: a colour handbook," *Australian Journal of Entomology*, vol. 44, no. 2, pp. 212–213, 2014.

[15] J. L. Zettler and F. H. Arthur, "Chemical control of stored product insects with fumigants and residual treatments," *Crop Protection*, vol. 19, no. 8, pp. 577–582, 2000.

[16] S. C. Hoyt, "Integrated chemical control of insects and biological control of mites on apple in washington," *Journal of Economic Entomology*, vol. 62, no. 1, pp. 74–86, 1969.

[17] S. Tang, J. Liang, Y. Tan, and R. A. Cheke, "Threshold conditions for integrated pest management models with pesticides that have residual effects," *Journal of Mathematical Biology*, vol. 66, no. 1-2, pp. 1–35, 2013.

[18] J. Liang, S. Tang, and R. A. Cheke, "An integrated pest management model with delayed responses to pesticide applications and its threshold dynamics," *Nonlinear Analysis Real World Applications*, vol. 13, no. 5, pp. 2352–2374, 2012.

[19] J. R. Beddington, C. A. Free, and J. H. Lawton, "Characteristics of successful natural enemies in models of biological control of insect pests," *Nature*, vol. 273, no. 5663, pp. 513–519, 1978.

[20] K. D. Lafferty and A. M. Kuris, "Biological control of marine pests," *Ecology*, vol. 77, no. 7, pp. 1989–2000, 1996.

[21] M. R. E. C., "Biological control of weeds," *Annual review of entomology*, vol. 43, no. 1, pp. 369–393, 1998.

[22] R. C. McFadyen *et al.*, "Successes in biological control of weeds," vol. 3, pp. 3–14, 2000.

[23] F. G. Howarth, "Environmental impacts of classical biological control," *Annual Review of Entomology*, vol. 36, no. 36, pp. 485–509, 1991.

[24] D. Simberloff and P. Stiling, "How risky is biological control?" *Ecology*, vol. 79, no. 5, pp. 1834–1836, 1998.

[25] S. Tang, G. Tang, and R. A. Cheke, "Optimum timing for integrated pest management: modelling rates of pesticide application and natural enemy releases," *Journal of Theoretical Biology*, vol. 264, no. 2, pp. 623–638, 2010.

[26] C. Xiang, Z. Xiang, and Y. Yang, "Dynamic complexity of a switched host-parasitoid model with beverton-holt growth concerning integrated pest management," *Journal of Applied Mathematics*, vol. 2014, no. 3, pp. 688–703, 2014.

[27] C. Xiang, Z. Xiang, S. Tang, and J. Wu, "Discrete switching host-parasitoid models with integrated pest control," *International Journal of Bifurcation and Chaos*, vol. 24, no. 9, p. 1450114, 2014.

[28] M. Doebeli, "Genetic variation and persistence of predator-prey interactions in the nicholson-bailey model," *Journal of Theoretical Biology*, vol. 188, no. 1, pp. 109–120, 1997.

[29] E. Liz, "A global picture of the gamma-ricker map: A flexible discrete-time model with factors of positive and negative density dependence," *Bulletin of Mathematical Biology*, vol. 80, no. 2, pp. 417–434, 2018.

[30] W. Qin, S. Tang, C. Xiang, and Y. Yang, "Effects of limited medical resource on a filippov infectious disease model induced by selection pressure," *Applied Mathematics & Computation*, vol. 283, no. C, pp. 339–354, 2016.

[31] Y. Yang and X. Liao, "Filippov hindmarsh–rose neuronal model with threshold policy control," *IEEE transactions on neural networks and learning systems*, vol. 30, no. 1, pp. 306–311, 2018.

[32] W. Qin, X. Tan, X. Shi, J. Chen, and X. Liu, "Dynamics and bifurcation analysis of a filippov predator-prey ecosystem in a seasonally fluctuating environment," *International Journal of Bifurcation and Chaos*, vol. 29, no. 2, p. 1950020, 2019.

[33] L. Nátr, "Murray, jd: Mathematical biology. i. an introduction." *Photosynthetica*, vol. 40, no. 3, pp. 414–414, 2002.

[34] S. Elaydi, *An Introduction to Difference Equations*. Springer, New York, 2005.

[35] T. Yuan, L. Pang, and T. Zhang, "Permanence, almost periodic oscillations and stability of delayed predator-prey system with general functional response," *IAENG International Journal of Applied Mathematics*, vol. 49, no. 2, pp. 155–164, 2019.

[36] B. Chen, "The influence of density dependent birth rate to a commensal symbiosis model with holling type functional response," *Engineering Letters*, vol. 27, no. 2, pp. 295–302, 2019.

[37] L. Liu, C. Xiang, and G. Tang, "Dynamics analysis of periodically forced filippov holling ii prey-predator model with integrated pest control," *IEEE Access*, vol. 7, pp. 113 889–113 900, 2019.

[38] Z. Xiao and Z. Li, "Stability and bifurcation in a stage-structured predator-prey model with allee effect and time delay," *IAENG International Journal of Applied Mathematics*, vol. 49, no. 1, pp. 6–13, 2019.